Phytochemical Profiling and Biological Testing of the Constituents of the Australian Plant Haemodorum brevisepalum

Norman, Edward; Hombsch, Stuart; Lever, James; Brkljaca, Robert; White, Jonathan; Gasser, Robin B.; Taki, Aya

Norman, E., Hombsch, S., Lever, J., Brkljaca, R., White, J., Gasser, R. B., Taki, A., & Urban, S. (2021). Phytochemical Profiling and Biological Testing of the Constituents of the Australian Plant Haemodorum brevisepalum. Journal of Natural Products, 84(11), 2832–2844.
https://doi.org/10.1021/acs.jnatprod.1c00509
Document Version: Accepted Manuscript

Published Version: https://doi.org/10.1021/acs.jnatprod.1c00509

Phytochemical Profiling and Biological Testing of the Constituents of the Australian Plant *Haemodorum brevisepalum*

Edward Owen Norman,[†] Stuart Hombsch,[†] James Lever,[†] Robert Brkljača,[§] Jonathan White,[‡] Robin B. Gasser,[⊥] Aya C. Taki,[⊥] and Sylvia Urban*[†]

[†] School of Science, Applied Chemistry and Environmental Science, RMIT University, GPO Box 2476 Melbourne, Victoria 3001, Australia

[§] Monash Biomedical Imaging, Monash University, Clayton, Victoria, 3168, Australia

[‡] School of Chemistry and Bio21 Institute, The University of Melbourne, Victoria 3010, Australia

[⊥] Department of Veterinary Biosciences, Melbourne Veterinary School, Faculty of Veterinary and Agricultural Sciences, The University of Melbourne, Parkville, Victoria 3010, Australia

ABSTRACT: Phytochemical profiling was undertaken on the crude extracts of the bulbs, stems and the fruits of *Haemodorum brevisepalum*, to determine the nature of the chemical constituents present. This represents the first study to investigate the fruits of a species of *Haemodorum*. In total, 13 new and 17 previously reported compounds were isolated and identified. The new compounds were of the phenylphenalenone-type class, with a representative of a novel structural form, named tentatively "oxabenzochromenone" (**1**), a compound akin to an intermediate in a recently proposed phenylphenalenone metabolic network (**2**), seven new phenylphenalenones (**4**–**10**), four new phenylbenzoisochromenones (**11**–**14**), and a new phenylbenzoisochromenone-derivative (**18**). The previously reported compounds identified were of the following structure classes: oxabenzochrysenone (**3**, **23**–**26**), flavonol (**15** and **16**), phenylbenzoisochromenone (**17**, **21**, **22**, **27**–**30**), and phenylphenalenone (**19**, **20**). Compounds **2**–**4**, **6**–**9**, **15**–**18**, **21**, **22** and **26** were subjected to antimicrobial evaluation with moderate activity observed against *Staphylococcus aureus* MRSA, and slight activity against *Pseudomonas aeruginosa* and *Candida albicans*. Compounds **4**, **6**–**9**, **17** and **21** were also evaluated for anthelminthic activity against larvae of the blood-feeding parasitic nematode, *Haemonchus contortus*.

Haemodoraceae is a family of monocotyledonous plants distributed across the temperate and tropical regions of the southern hemisphere.[1] The family has proven to be a rich source of phenylphenalenone-type specialized metabolites, which conform to four general groups: phenylphenalenones (PhP), oxabenzochrysenones (OBC), phenylbenzoisochromenones (PBIC), and the phenylbenzoisoquinolinediones (PBIQ) (Figure 1).[2] To date, 145 PhP-type compounds have been isolated from Haemodoraceae, of which 20 originate from the genus *Haemodorum*.[2] *Haemodorum* spp., commonly known as "bloodroots", have documented ethnomedicinal uses. For instance, they have been employed by the Aboriginal People of Australia as a remedy for dysentery (*H. spicatum*) as well as a treatment for bites and stings (*H. corymbosum*).[3]

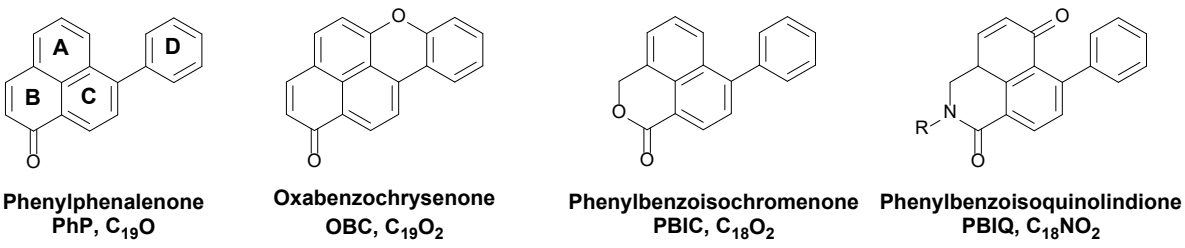

Figure 1. Overview of the principal phenylphenalenone-type structure classes (and their abbreviations).

PhP-type specialized metabolites are biologically active, functioning as a form of chemical defense within the family of plants belonging to Haemodoraceae, as either phytoalexins or phytoanticipins.[2] This bioactivity arises primarily as a result of the phototoxic properties of the highly conjugated nucleus common across the class.[4, 5] Structure-activity-relationship (SAR) studies have determined that, with appropriate functionalization, the phenalenone nucleus can achieve comparable efficacy to industry-standard antifungal agents, such as benomyl and propiconazole, against the plant pathogen *Mycosphaerella* (*Pseudocercospora*) *fijiensis*.[5] As

such, the continued discovery of unique PhP-type compounds is of significance to the broader scientific community as part of the fight against drug-resistant pathogens or superbugs.[6]

The Marine and Terrestrial Natural Product (MATNAP) research group at RMIT University has been investigating members of the genus *Haemodorum* since 2009 (*H. simplex*, which subsequently underwent taxonomic revision to *H. simulans*, as well as *H. spicatum*).[7-9] As part of our continuing efforts to profile plants of the *Haemodorum* genus, the present investigation involved a comprehensive phytochemical screening of the previously unstudied Australian endemic plant, *H. brevisepalum*. The decision to study this plant was based on its rarity, in that it only occurs in a small range in the south-west botanical province of Western Australia, appearing and blooming only after a bushfire.[10] This is also the first instance in which the fruits of a member of *Haemodorum* have been chemically profiled.

As part of the current study, a new grouping of PhP-related compounds, tentatively assigned as the oxabenzochromenone (OBC) class, was identified with the discovery of the new natural product **1** (Table 1). A recently proposed metabolic network in the genus *Xiphidium* (Haemodoraceae) could be substantiated via the isolation of the naturally occurring compound **2**, from *Haemodorum* (Table 2 and S1, Supporting Information).[11,12] The single-crystal structure of a previously reported member of the OBC class **3** was secured for the first time, representing only the second instance of any OBC yielding an X-ray crystal structure (Figure 2 and S2–S3, Supporting Information).[13] Overall, this study resulted in the isolation and identification of 13 new natural products, the formation of a new structural derivative, as well as the isolation of 17 previously identified compounds. The new compounds were of the phenylphenalenone-type class including a representative (**1**) of a novel structural form tentatively named "oxabenzochromenone", an unreported carboxyphenylnapthoquinone intermediate in the phenylphenalenone biosynthetic network (**2**), seven new phenylphenalenones (**4**–**10**) and four new phenylbenzoisochromenones (**11**–**14**) as well as the

new phenylbenzoisochromenone derivative (**18**). The complete NMR spectra for the 13 unreported compounds and the derivative are presented in Figures S4–S133, Supporting Information. The 17 previously reported compounds were identified as follows: four oxabenzochrysenone aglycones - 5-methoxy-1*H*-naptho[2,1,8-*mna*]xanthen-1-one (**3**),[9] 5-hydroxy-1*H*-naptho[2,1,8-*mna*]xanthen-1-one (**23**),[9] 5-hydroxy-2-methoxy-1*H*-naptho[2,1,8-*mna*]xanthen-1-one (**24**),[9] and 2,5-dimethoxy-1*H*-naptho[2,1,8-*mna*]xanthen-1-one (**25**),[9] an oxabenzochrysenone glycoside - haemodoroxychrysenose (**26**),[8] two flavonol glycosides - quercetin-3-*O*-*β*-D-glucopyranoside (**15**),[14] and quercetin-3-*O*-[*β*-D-glucopyranosyl-(1→6)-*β*-D-glucopyranoside] (**16**),[15] three phenylbenzoisochromenone glycosides - 5-hydroxy-6-*O*-(*β*-D-glucopyranosyl)-7-phenyl-3*H*-benzo[*de*]isochromen-1-one (**17**),[16] 6-*O*-(*β*-D-glucopyranosyl)-(3*R/S*)-3,5-dihydroxy-7-phenyl-3*H*-benzo[*de*]isochromen-1-one (**21**),[17] and 6-*O*-(*β*-D-glucopyranosyl)-(3*R/S*)-3-carboxy-5-hydroxy-7-phenyl-3*H*-benzo[*de*]isochromen-1-one (**22**),[17] four phenylbenzoisochromenone aglycones - haemodordiol (**27**),[9] 6-hydroxy-(3*R/S*)-3,5-dimethoxy-7-phenyl-3*H*-benzo[*de*]isochromen-1-one (**28**),[18] 5-hydroxy-(3*R/S*)-3,6-dimethoxy-7-phenyl-3*H*-benzo[*de*]isochromen-1-one (**29**),[19] and haemodorone (**30**),[7] as well as two phenylphenalenone glycosides - lachnanthoside (**19**),[20] and dilatrin (**20**).[20] Finally, any isolated compounds obtained in sufficient mass quantities and stability were evaluated for their antimicrobial and anthelmintic activity, with moderate activity observed against *Staphylococcus aureus* MRSA and slight activity observed against *Pseudomonas aeruginosa* and *Candida albicans* (Figure S134, Supporting Information). No anthelmintic activity was detected for any of the compounds tested.

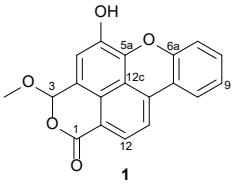

1

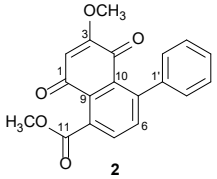

2

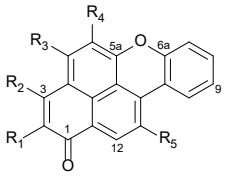

3 R_4 = OH, R_1, R_2, R_3, R_5 = H
23 R_4 = OCH$_3$, R_1, R_2, R_3, R_5 = H
24 R_1 = OH, R_4, R_2, R_3, R_5 = H
25 R_1, R_4 = OCH$_3$, R_2, R_3, R_5 = H
26 R_4 = OCH$_3$, R_5 = Pyr, R_1, R_2, R_3 = H

Oxabenzochrysenones (OBC)

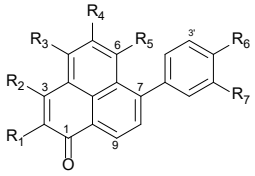

4 R_1, R_4 = OCH$_3$, R_5 = Pyr-Pyr-Caff, R_2, R_3 = H
5 R_1 = Pyr, R_4 = OH, R_5 = Pyr-2-Pyr, R_2, R_3 = H
6 R_4 = Pyr-6-Pyr, R_1, R_2, R_3, R_5 = H
7 R_4 = OH, R_1 = Pyr, R_2, R_3, R_5 = H
19 R_1, R_4 = OCH$_3$, R_5 = OH, R_2 = Pyr, R_3, R_6 = H
20 R_1 = OCH$_3$, R_4 = OH, R_5 = Pyr, R_2, R_3, R_5 = H

7-Phenylphenalenones (7-PhP)

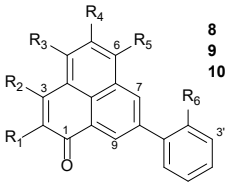

8 R_4, R_6 = OH, R_5 = Pyr, R_1, R_2, R_3 = H
9 R_1, R_6 = Pyr, R_5 = OH, R_2, R_3, R_4 = H
10 R_4, R_5 = OH, R_6 = Pyr, R_1, R_2, R_3 = H

8-Phenylphenalenones (8-PhP)

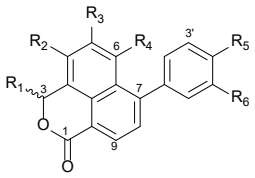

17 R_3 = OH, R_1 = Pyr, R_2, R_5, R_6 = H
21 R_1, R_4 = COOH, R_3 = OH, R_2 = Pyr, R_5, R_6 = H
22 R_1 = OCH$_3$, R_3 = OH, R_2, R_5, R_6 = H
27 R_1 = OCH$_3$, R_3, R_4 = OH, R_2, R_5, R_6 = H
28 R_1, R_3 = OCH$_3$, R_4 = OH, R_2, R_5, R_6 = H
29 R_1, R_4 = Carbonyl, R_3 = OH, R_2 = OCH$_3$, R_5, R_6 = H
30 R_1 = OCH$_3$, R_4 = OH, R_2, R_3, R_5, R_6 = H

7-Phenylbenzoisochromenones (7-PBIC)

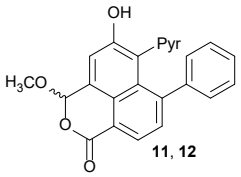

11, **12**

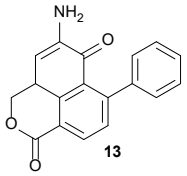

13

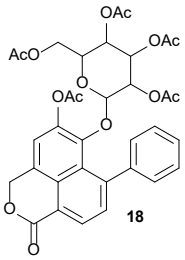

18

7-Phenylbenzoisochromenone (7-PBIC, Acetylated Derivative)

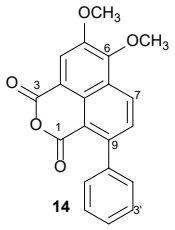

14

9-Phenylbenzoisochromenone (9-PBIC)

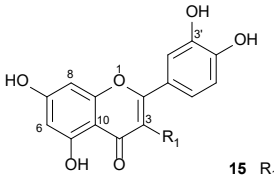

15 R_1 = Pyr
16 R_1 = Pyr-6-Pyr

Flavonoids

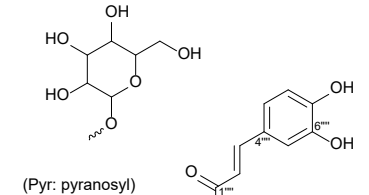

(Pyr: pyranosyl)
(Pyr-Pyr-Caff: pyranosyl-(2->1)-pyranosyl-(6->1)-caffeoyl)

Glycoside R-Groups

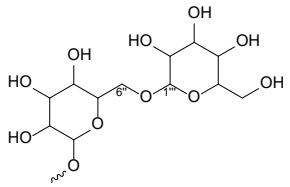

(Pyr-6-Pyr: pyranosyl-(6->1)-pyranosyl)

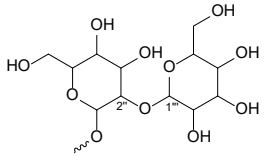

(Pyr-2-Pyr: pyranosyl-(2->1)-pyranosyl)

Table 1. 2D NMR Data (500 MHz, CD_3OD) of Compound **1**[a]

Position	Carbon, type[b]	Proton, mult. (*J* in Hz)	gCOSY	gHMBCAD
1	164.2, C			
3	102.6, CH	6.45, s	4[c]	1, OCH_3-3, 12b
3a	ND			
4	119.2, CH	7.35, s	3[c]	5a, 12b
5	ND			
5a	137.6, C			
6a	152.7, C			
7	117.4, CH	7.28, d (7.5)	8	
8	131.5, CH	7.43, dd (7.5, 7.5)	7, 9, 10[c]	
9	123.9, CH	7.22, dd (7.5, 8.0)	8, 10	7, 10a
10	123.5, CH	8.02, d (8.0)	9	6a, 8
10a	119.3, C			
10b	132.4, C			
11	113.8, CH	7.77, d (8.0)	12	10a, 12a, 12c
12	128.2, CH	8.07, d (8.0)	11	10b
12a	116.5, C			
12b	121.8, C			
12c	120.9, C			
OCH_3-3	54.8, CH_3	3.64, s		3

[a] Referenced to *CD_3OD*, 500 MHz.
[b] Carbon assignments based on HSQCAD and gHMBCAD NMR experiments.
[c] Indicates weak or long-range correlation.

Table 2. 2D NMR Data (500 MHz, CD_3OD) of Compound **2**[a]

Position	Carbon, type[b]	Proton, mult. (J in Hz)	gCOSY	gHMBCAD
1	180.2, C			
2	102.7, CH	6.11, s		1, 3, 4, 8, 9, 10[c],
3	168.6, C			
4	179.7, C			
5	146.9, C			
6	134.6, CH	7.48, d (8.0)	7	1′, 8, 10
7	132.2, CH	7.66, d (8.0)	6	6, 7, 8[w], 9, 11
8	132.0, C			
9	129.7, C			
10	128.8, C			
11	169.9, C			
1′	140.5, C			
2′/6′	127.7, CH	7.26, d (7.5)	3′/5′	3′/5′, 4′, 5
3′/5′	127.8, CH	7.38, m	2′/6′	2′/6′
4′	127.2, CH	7.38, m		
OCH_3-3	56.8, CH_3	4.02, s		3
OCH_3-11	51.9, CH_3	3.95, s		11

[a] Referenced to *$(CD_3)_2SO$*, 500 MHz.
[b] Carbon assignments based on HSQCAD and gHMBCAD NMR experiments.
[c] Indicates weak or long-range correlation.

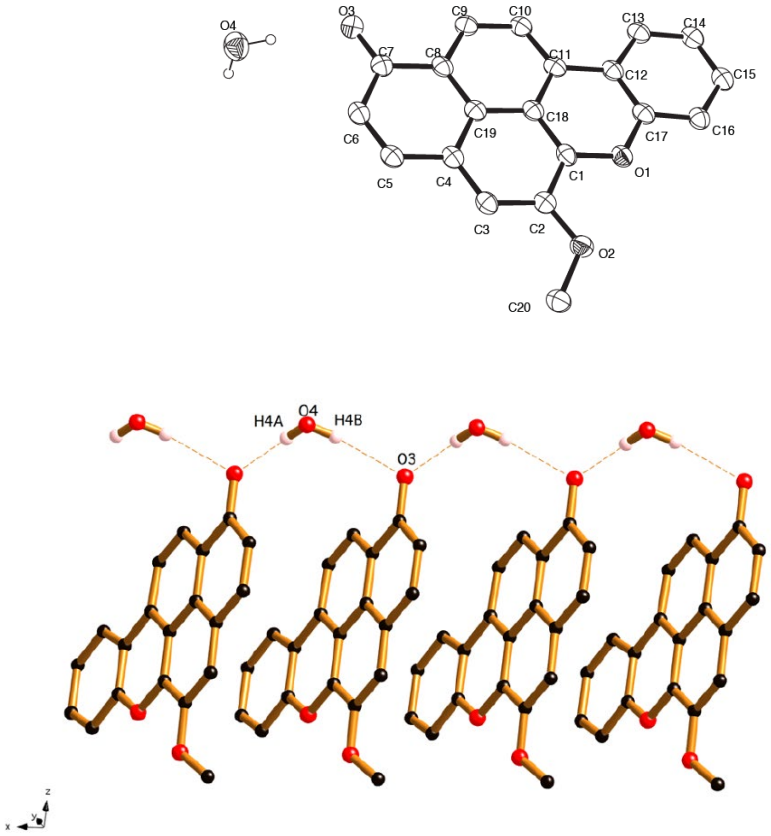

Figure 2. Top - thermal ellipsoid plot of compound **3**, Bottom – H-bond and π-stacking of compound **3**.

RESULTS AND DISCUSSION

The bulbs, stems and fruits of *H. brevisepalum* were extracted using 3:1 MeOH-CH_2Cl_2, evaporated under reduced pressure, and then sequentially solvent partitioned (triturated) into CH_2Cl_2- and MeOH-soluble fractions, respectively. Crude extracts were fractionated via column chromatography, with the CH_2Cl_2 and MeOH extracts subjected to flash silica gel column chromatography and C_{18} vacuum-liquid chromatography (VLC), respectively.

Analysis of the column-fractionated crude extracts via analytical HPLC suggested the presence of an abundance of characteristic UV profiles for three distinct compound classes,

typical of *Haemodorum* spp.[9] These characteristic UV profiles are indicative of the PhPs (λ_{max} >400 nm), OBCs (λ_{max} >500 nm) and PBICs (λ_{max} <400 nm), see Figures S135–S137, Supporting Information.[9] The λ_{max} values are used only as a guide to support the tentative structure class, since closely related compounds, such as the OBCO's are also possible, for example, compound **1**.[7-9, 21, 22] Diagnostic ^{13}C NMR chemical shifts for the carbonyl C-1 of the PhP (δ_C ~180), OBC (δ_C ~175) and PBIC (δ_C ~165) structure classes was supported by gHMBCAD correlations from nearby protons throughout the study (see Figures S138–S140, Supporting Information).

PhP-glycosides have become the chemotaxonomic marker of the Haemodoraceae, subfamily Haemodoroideae.[23] The steric hindrance of these bulky glycone moieties creates problematic spectroscopic effects, particularly in the determination and elucidation of pendant aromatic substitution, determining the relative configuration of the glycoside group moiety, as well as establishing the point of attachment of the glycone group moiety itself.[23] In a previous study,[23] it has been noted that the location of the sugar unit has been determined to typically reside at C-6 on the phenalenone nucleus in haemocorin, lachnanthoside, dilatrin, and a number of other PhP and PBIC glycosides. What was evident is that when PhP-glycosides are substituted at both C-5 and C-6, it is difficult to determine unequivocally the placement of the glycoside group moiety is at either C-5 or C-6 on the basis of NMR spectroscopy (Figure 3). Previous studies have either failed to mention how the placement was determined or have not adequately used NMR spectroscopic methods to determine the position of the attachment for the glycoside group moiety. This study employed a chemical derivatization (acetylation) followed by a combined HMBC/1D ROESY approach to assign these carbon shifts in 5,6-substituted PhP and PBIC glycosides (for the full details of the approach illustrated in Figure 3, see Figures S141–S145, Supporting Information). In this study the identity of the glycoside group moieties was confirmed by NMR spectroscopy. However, due to congestion of the ^{1}H NMR spectrum

in the sugar region (δ_H ~2.5-4.5), the relative configuration assignment was precluded via NOE enhancement experiments.

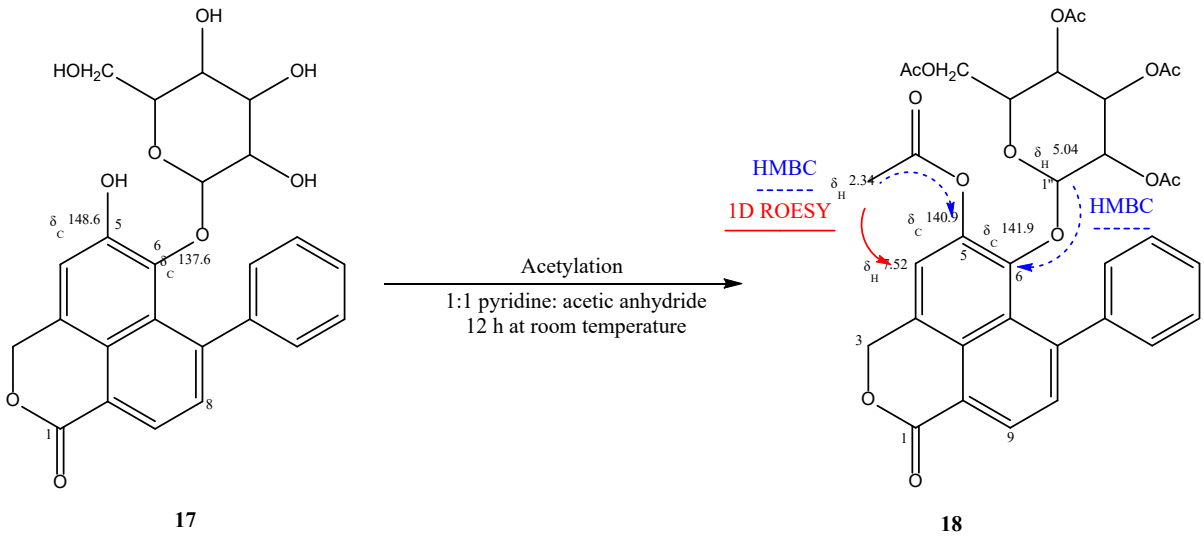

17 **18**

Figure 3. Approach to the determination of glycosidic group moiety location on 5,6-substituted PhP-type compounds.

The crude CH_2Cl_2 extract of the stems was separated via flash silica gel column chromatography to yield 20 fractions. The seventh silica gel fraction underwent further separation via Sephadex LH-20 size exclusion column chromatography to yield a further 20 fractions, the sixth to eighth of which were further separated via C_{18} solid-phase extraction (SPE) to produce 41 enriched fractions. Of these, fractions nine to 15 were combined and purified via semi-preparative RP-HPLC. There were seven peaks of interest in the fraction, yet only one peak had sufficient mass to enable structure elucidation to be undertaken (Figure S146, Supporting Information).

The first chromatographic peak (t_R = 35.40 min – **1**, see Figure S146, Supporting Information) was initially misleading, as it had a λ_{max} of 437 nm, which suggested a PhP class compound. After exhaustive attempts to reconcile the NMR spectroscopic data (Figures S4–

S7, Supporting Information), it became clear that this compound could not represent a PhP (Figure 1). It was noted that certain diagnostic shifts of both OBC (δ_{C5a} = 135-140 and δ_{C6a} = 150-155) and PBIC (δ_{C1} = 160-170) structure classes were present in this compound, (Figures S147–S149, Supporting Information).

This compound was finally elucidated as the new compound, 5-hydroxy-3-methoxy-3*H*-2,6-dioxabenzo[*def*]chrysen-1-one (**1**). The key 2D NMR (COSY and HMBC) correlations supporting the elucidation of compound **1** are shown in Figure 4. The proposed structure resulted in a molecular formula of $C_{19}H_{12}O_5$, supported via HRESIMS [observed *m/z* 319.0608 $[M - H]^-$ (calcd for $C_{19}H_{11}O_5$, *m/z* 319.0612)] (Figure S150, Supporting Information). Only one compound of this type has been reported previously and was grouped with the OBC compounds, yet this can be misleading as other members of this class invariably have λ_{max} >500 nm.[19] Here we propose a new group of PhP-type compounds tentatively designated as the "oxabenzochromenones" (given the abbreviation OBCO) to classify compounds such as **1**.

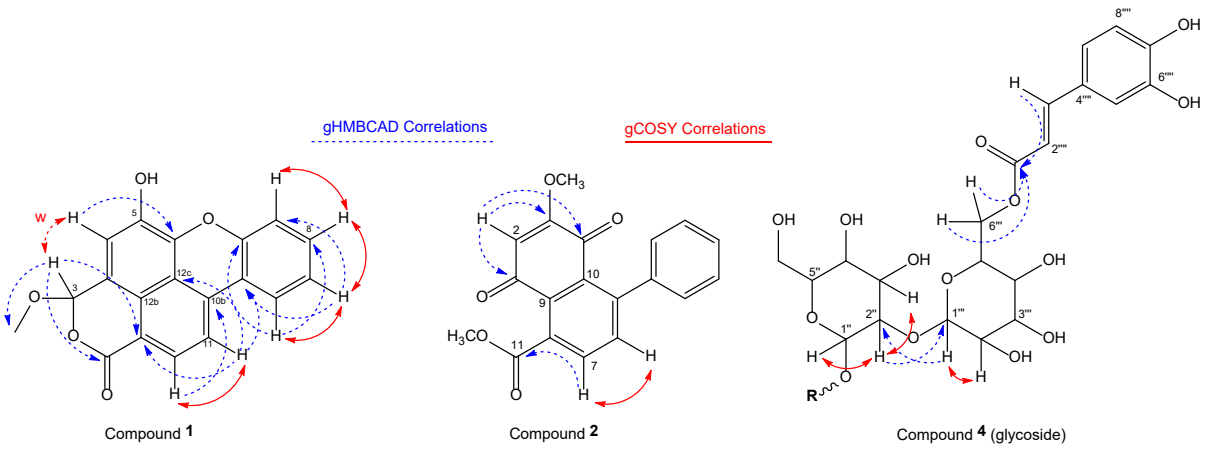

Figure 4. Key gHMBCAD and gCOSY NMR correlations supporting the elucidation of compounds **1**, **2**, and the glycoside group moiety of **4**.

The crude CH_2Cl_2 extract of the stems was separated via flash silica gel column chromatography to produce 20 fractions and the 14th and 15th fractions were combined and further separated by semi-preparative RP-HPLC purification, to yield five chromatographic peaks of interest. The ^1H and gHMBCAD NMR spectroscopic data of the fifth peak (t_R = 24.01 min – **2**, see Figures S8–S11 and S151, Supporting Information) did not conform with any of the typical PhP classes. In general, carbonyl-carbons are the only diagnostic feature within these classes that have δ_C >165 ppm. In this instance, compound **2**, which was responsible for this chromatographic peak, exhibited four signals above δ_C 165 ppm (δ_C 168.6, 169.9, 179.7 and 180.2 ppm) that are uncommon in PhP-type compounds. The proton signal at δ_H 6.11 showed HMBC correlations to three of these deshielded carbons (δ_C 168.6, 179.7 and 180.2 ppm, see Figure S152, Supporting Information). After careful consideration, it was determined that this compound may be of a different class altogether rather than any PhP-type compound that had been observed thus far in this study.

After further inspection of the NMR spectroscopic data of **2**, alongside previously studied compounds such as the PBIC anhydrides **14** and **30**, which had similar NMR spectroscopic data, it was evident that if the ester bond formed from the terminal oxygen of the lactone group moiety present in PBICs is cleaved between O-2 and C-3, the resulting compound would lead to the required number of downfield carbon signals (Figure 4 and Figure S1, Supporting Information).The elucidation of this compound was achieved by positioning one proton at δ_H 6.11 (s), isolated on an aromatic ring (C-2) that correlated via HMBC to three downfield carbons (C-1, C-3 and C-4 with δ_C 180.2, 168.6 and 179.7, respectively) and a proton δ_H 7.66 (d, J = 8.0 Hz) as part of an aromatic spin system (C-7) correlated via HMBC to an isolated downfield carbonyl carbon (C-11 with δ_C 169.9). The proposed structure resulted in a molecular formula of $C_{19}H_{14}O_5$, confirmed via HRESIMS [observed *m/z* 323.0912 $[M + H]^+$ (calcd for $C_{19}H_{15}O_5$, *m/z* 323.0919)] (Figure S153, Supporting Information).

This compound was elucidated as methyl 3-methoxy-5-phenyl-1,4-dihydronapthoquinone-8-carboxylate (**2**). Of interest here is the similarity between compound **2**, and the carboxyphenylnapthoquinone isolated in a recent paper documenting a proposed phenylphenalenone metabolic network in the genus *Xiphidium* (Haemodoraceae) (Figure S1, Supporting Information).[12,17] The ring opening of a PBIC was first demonstrated in 2002 by Opitz et al., who treated a PBIC with diazomethane.[19] In 2019, a carboxyphenylnapthoquinone was isolated from *Xiphidium caeruleum*, and, in this study, compound **2** was isolated from the genus *Haemodorum*, bearing methoxy group moieties that are likely artefactual from the use of methanol as an extraction solvent. This suggests that aside from the *Lachnanthes*, *Schiekia*, *Wachendorfia*, and *Xiphidium* genera, PBIQ alkaloids and phenylcarbamoylnapthoquinones (PCNQs) may also be present in *Haemodorum*.[2, 12, 17]

The HPLC chromatogram of the eighth fraction of the methanolic extract of the bulbs exhibited a number of chromatographic peaks with a λ_{max} of 525 nm, suggesting OBCs were present within this fraction (Figure S154, Supporting Information).[9] The major component of this fraction (t_R = 17.32 min – **3**, see Figure S155, Supporting Information) was isolated and subsequently elucidated via dereplication, primarily on the basis of comparison with other known OBCs isolated throughout this study (**23**–**26**), and reported previously in the literature.[7-9, 21] Its identity was determined as the previously reported oxabenzochrysenone, 5-methoxy-1*H*-naphtho[2,1,8-*mna*]xanthen-1-one (**3**).[9] Of interest was the fact that this purified compound crystallized as thin orange plates upon refrigeration at -20 °C. Access to the X-Ray crystallographic analysis facilities at the Australian Synchrotron allowed for the single-crystal structure of **3** to be obtained for the first time, see Figure 2 (for details of atomic co-ordinates and hydrogen bonds for **3** see Figure S2–S3, Supporting Information).

The methanolic extract of the bulbs was fractionated via C_{18} VLC to yield twelve fractions. The fifth fraction exhibited a number of chromatographic peaks with a λ_{max} of 465–475 nm,

suggesting PhPs were present within this fraction (Figure S156, Supporting Information).[9] This fraction was further purified via semi-preparative RP-HPLC. The major component contained in this fraction (t_R = 11.47 min – **4**, see Figure S157, Supporting Information) was isolated and subsequently elucidated, primarily via 1D and 2D NMR experiments (Figures S24–S335, Supporting Information). Low-resolution electrospray ionization mass spectrometry (LRESIMS) together with HRESIMS supported the molecular mass proposed by the elucidation that follows (Figures S158–S159, Supporting Information). The overall ^{1}H NMR spectrum was similar to other previously described 2,5,6-substituted 7-PhPs isolated in other studies (Figure S24, Supporting Information).[7-9, 21, 22] The pendant aromatic ring was positioned at C-7, due to the diagnostic doublets observed at C-8 and C-9 (δ_H 7.51 and 8.21, respectively), with key gHMBCAD correlations observed between the proton at C-9 (δ_H 8.21) and the carbonyl carbon at C-1 (δ_C 179.9), as well as between the proton at C-8 (δ_H 7.51) and the aromatic quaternary carbon at C-1′ (δ_C 143.6) (Figures S160-162, Supporting Information). Two methoxy group moieties were placed at C-2 and C-5, due to two clear gHMBCAD correlations from OCH_3-2 (δ_H 3.84) to C-2 (δ_C 151.9) and from OCH_3-5 (δ_H 3.54) to C-5 (δ_C 147.4) (Figures S163-164, Supporting Information). This was further substantiated by additional correlations being observed from the singlet protons located at C-3 and C-4 (δ_H 6.84 and 7.34, respectively), leaving an undetermined substituent remaining at C-6. At this point, attention was drawn to the remaining spectroscopic signals, as well as the uncommon molecular ion obtained for this compound via LRESIMS at *m/z* 817 $[M - H]^-$, significantly higher than previously observed for glycosidic PhP-type compounds, which range from 400-500 amu.[7-9, 21, 22]

The presence of a complex glycoside group moiety was supported by the protons clustered in the region between δ_H 2.5-4.5 in the ^{1}H NMR spectrum, the presence of two anomeric protons at δ_H 4.19 (d, J = 7.5 Hz) and 4.49 (d, J = 7.5 Hz), as well as two negatively phased

contours in this region of the HSQCAD NMR spectrum. The latter indicated the presence of two methylene environments, suggesting the presence of a disaccharide group moiety (Figure S165, Supporting Information). The remaining mass difference was accounted for due to the presence of two diagnostic, correlated doublets that are uncommon among other PhPs of this type, located at δ_H 6.99 (d, J = 16 Hz) and δ_H 5.35 (d, J = 16 Hz) (Figure S166, Supporting Information). This spin-system is indicative of *trans*-oriented olefinic protons, and via gHMBCAD experiments, it was determined that these olefinic signals, combined with the glycosidic signals, resulted in a 2″- 1‴ linked disaccharide with a further caffeoyl group moiety attached at the 6‴-*O* end of the disaccharide. Deviation from the typical *β*-(1->4) arrangement of this disaccharide prompted further consideration, with the key 2D NMR experimental correlations for the elucidation of the glycosidic group moiety for compound **4** shown in Figure 4.

The previously detailed elucidation is typical of a 2,5-dimethoxy-7-phenylphenalen-1-one, and together with the 6-*O*-glycoside group moiety just described, this resulted in a molecular formula of $C_{42}H_{42}O_7$, supported via HRESIMS [observed *m/z* 817.2341 $[M - H]^-$ (calcd for $C_{42}H_{41}O_7$, *m/z* 817.2344)] (Figure S159, Supporting Information). The structure for compound **4** was, therefore, determined to be (6-((2-((2,5-Dimethoxy-1-oxo-7-phenyl-1*H*-phenalen-6-yl) oxy)-4,5-dihydroxy-6-(hydroxymethyl)tetrahydro-2*H*-pyran-3-yl)oxy)-3,4,5-trihydroxytetrahydro-2*H*-pyran-2-yl) methyl (*E*)-3-(3,4-dihydroxyphenyl) acrylate and represents a new natural product. The ^{1}H and ^{13}C NMR spectroscopic data for all remaining unreported PhPs (**4**–**10**) are presented in Tables 3 and 4.

Table 3. ^{13}C NMR Spectroscopic Data of Compounds **4-10** (125 MHz, CD_3OD)[a]

no.	4	5	6	7	8	9	10
1	179.9	180.4	180.7	ND	186.7	180.5	186.6
2	151.9	152.1	151.1	ND	127.4	149.0	127.3
3	113.1	113.7	114.1	114.1	142.2	115.1	142.5
3a	126.3	125.7	130.6	ND	128.1	124.8	ND
4	123.1	123.4	121.2	121.4	124.9	131.0	125.0
5	147.4	147.2	156.1	ND	147.9	109.7	146.5
6	140.1	139.9	110.8	111.1	142.3	155.5	145.2
6a	129.9	ND	126.8	ND	128.8	122.4	ND
7	146.3	146.3	148.1	145.3[c]	129.3	130.3	130.8
8	130.4	130.7	127.8	128.0	138.4	137.3	ND
9	127.3	127.5	128.0	128.1	129.8	132.6	131.5
9a	120.7	127.8	131.2	ND	125.2	131.3	127.0
9b	127.5	120.6	121.1	ND	121.2	123.3	123.0
1′	143.6	144.1	130.4	131.0	127.3	127.2	ND
2′	125.7-131.0	126.5-130.3	115.0	119.3	154.3	115.7	ND
3′	125.7-131.0	126.5-130.3	131.3	147.8[c]	115.8	129.0	115.9
4′	125.7-131.0	126.5-130.3	157.8	ND[c]	129.0	119.8	ND
5′	125.7-131.0	126.5-130.3	131.3	116.0	119.9	130.8	120.0
6′	125.7-131.0	126.5-130.3	115.0	125.4	130.7	154.3	130.7
1″	102.0	100.6	100.9	101.4[b]	106.4	100.5	ND
2″	85.7	83.0	73.3	73.3[b]	74.1	73.4	73.7
3″	74.8	75.4	76.5	76.5[b]	76.5	76.6	ND
4″	69.8	69.6	69.4	69.3[b]	69.4	69.9	ND
5″	76.1	76.3	76.6	76.6[b]	77.2	77.0	ND
6″	61.1	61.0	60.5	60.3[b]	60.8	61.1	61.1[c]
1‴	106.4	104.5		102.7[b]			103.9
2‴	74.5	74.0		73.5[b]			74.4
3‴	76.0	76.3		76.1[b]			ND
4‴	70.4	69.8		69.7[b]			ND
5‴	75.5	77.3		76.8[b]			ND
6‴	64.5	60.8		60.7[b]			60.7[c]
1⁗	167.4						
2⁗	112.2						
3⁗	144.7						
4⁗	125.3						
5⁗	109.6						
6⁗	149.0						
7⁗	147.3						
8⁗	114.8						
9⁗	121.9						
OCH_3-2	54.6	54.8					
OCH_3-6	54.5						

[a] Carbon assignments based on HSQCAD and gHMBCAD NMR experiments.
[b] Assignments for entire sugar moieties interchangeable.
[c] Indicates signals interchangeable.

Table 4. ^{1}H NMR Spectroscopic Data of Compounds **4-10** (500 MHz, CD_3OD)

no.	4	5	6	7	8	9	10
2					6.63, d (10.0)		6.67, d (9.5)
3	6.85, s	7.15, s	7.01, s	7.10, s	7.85, d (10.0)	7.03, s	7.94, d (10.0)
4	7.35, s	7.59, s	7.48, s	7.57, s	7.59, s	7.56, d (8.0)	8.05, s
5						7.18, d (8.0)	
6			7.57, s	7.67, s			
7					9.01, d (2.0)	8.93, d (1.5)	
8	7.52, d (7.5)	7.56, d (8.0)	7.63, d (7.5)	7.74, d (8.0)			8.80, d (1.5)
9	8.22, d (7.5)	8.49, d (7.5)	8.44, d (7.5)	8.53, d (7.5)	8.75, d (2.0)	8.90, d (1.5)	8.94, d (2.0)
2′	7.44-7.47, m	7.25-7.61, m	6.97, d (8.0)	7.38, d (1.5)		6.97, m	
3′	7.44-7.47, m	7.25-7.61, m	7.35, d (8.0)		6.97, d (7.5)	7.25, ddd (1.5, 8.0, 8.0)	6.99, d (7.5)
4′	7.44-7.47, m	7.25-7.61, m			7.24, ddd (1.5, 7.5,	6.99, m	7.26, dd (9.0, 8.0)
5′	7.44-7.47, m	7.25-7.61, m	7.36, d (8.0)	7.04, d (8.0)	6.99, dd (7.5, 7.5)	7.45, dd (1.5, 7.5)	7.00, d (6.5)
6′	7.44-7.47, m	7.25-7.61, m	6.96, d (8.0)	7.14, dd (1.5, 8.0)	7.50, dd (1.5, 7.5)		7.47, d (7.5)
1″	4.49, d (7.5)	4.90, d (8.0)	4.94, d (7.0)	4.92, d (7.5)	4.88. d (8.5)	5.18, d (7.5)	5.10, d (8.0)
2″	2.45, dd (8.0, 9.0)	2.38, dd (8.0, 9.0)	3.50, m	3.49, m	3.68, dd (9.0, 8.5)	3.64, dd (7.5, 9.0)	3.64, m
3″	3.34, m	3.36, m	3.48, m	3.45, m	3.47, dd (9.0, 9.0)	3.48, dd (9.0, 9.0)	3.16-3.77, m
4″	2.98, t (9.0)	3.09, dd (9.0, 9.5)	3.49, m	3.49, m	3.54, dd (9.0, 9.5)	3.44, dd (9.0, 9.0)	3.16-3.77, m
5″	2.80, m	2.89, m	3.32, m	3.30, m	3.34, m	3.53, m	3.16-3.77, m
6″a	3.49, m	3.53, dd (2.5, 11.5)	3.76, d (2.5)	3.80, m	3.78, dd (2.0, 12.5)	3.74, dd (5.0, 11.5)	3.76, m[a]
6″b	3.42, dd (6.0, 12.0)	3.45, dd (5.5, 11.5)	3.76, d (2.5)	3.74, m	3.85, dd (4.5, 12.5)	3.93, dd (1.5, 11.5	3.76, m[a]
1‴	4.19, d (8.0)	4.22, d (7.5)		4.87, m			5.42, d (8.0)
2‴	3.31, m	3.26, dd (8.0, 9.0)		3.55, m			3.68, m
3‴	3.47, m	3.39, m		3.46, m			3.16-3.77, m
4‴	3.26, t (9.5)	3.37, m		3.43, m			3.16-3.77, m
5‴	3.79, t (9.0)	3.31, m		3.36, m			3.16-3.77, m
6‴a	4.40, d (12.0)	3.79, dd (2.0, 12.0)		3.80, m			3.70, m[a]
6‴b	4.32, dd (8.5, 12.0)	3.68, dd (5.0, 12.5)		3.66, m			3.63, m[a]
2⁗	5.36, d (16.0)						
3⁗	6.99, d (16.0)						
5⁗	6.28, s						
8⁗	6.45, d (8.0)						
9⁗	6.21, d (8.0)						
OCH_3-2	3.84, s	3.93, s					
OCH_3-6	3.54, s						

[a] Indicates signals interchangeable.

The crude methanolic extract of the stems was separated via C_{18} VLC to yield ten fractions. The fifth fraction was prioritized due to the presence of characteristic PhP chromophores (λ_{max} in the range of 300-600 nm), signals of interest in the ^{1}H NMR spectrum, and the greater mass of this fraction compared to the other fractions. This fraction was further separated via Sephadex LH-20 size exclusion column chromatography resulting in fifteen enriched fractions. Fractions four to six were combined and subsequent semi-preparative HPLC contained eight chromatographic peaks of interest, of which several exhibited a λ_{max} of 367 nm, indicative of the PBIC structure class (Figure S167, Supporting Information).

These suspected PBIC-compounds displayed diagnostic NMR chemical shifts, which when compared with literature data, suggested the identities of three of the compounds as the previously reported PBICs **17**, **21** and **22** (Figures S168–S170, Supporting Information).[7-9, 21] The chromatographic peak at (t_R = 16.32 min – **11** and **12**, see Figure S171, Supporting Information) subsequently was confirmed to represent two co-eluting compounds as represented in the ^{1}H NMR spectrum (Figure S94, Supporting Information). These were identified as the new natural products **11** and **12** with a methoxy group moiety at C-3 (*R* and *S*), whereby the two compounds were suspected to differ in their in their configuration (diastereomers) at this position as the singlet peak could be resolved into two discrete singlet signals detected at δ_H 3.683 and δ_H 3.679 for the methoxy group moieties, respectively (Tables 5, 6 and Figure S172, Supporting Information). This hypothesis was supported further by the presence of two discrete proton signals from the C-3 proton at δ_H 6.46 (**11**) and 6.45 (**12**), which could be differentiated in the HSQCAD spectrum, coupling to C-3 (δ_C 102.1 and 102.0, respectively; see Tables 5, 6 and Figure S173–S174, Supporting Information) These discrete singlets showed gHMBCAD correlations to C-1 (δ_C 164.7), OCH_3-3 (δ_C 55.2) and weakly to C-9b (δ_C 123.1) (Figure S175, Supporting Information).

The anomeric protons of the sugars attached to the two compounds **11** and **12**, despite falling very close to the solvent peak in the HSQCAD spectrum, were also discernible (compound **11**: δ_H 4.77 and δ_C 102.4, and compound **12**: δ_H 4.72 and δ_C 102.6; see Figure S176, Supporting Information). Unfortunately, this mixture was isolated in such a small quantity (0.4 mg) that it was not possible to differentiate and further resolve or separate the C-3 (*R/S*) **11** and **12** diastereomers.

Table 5. ^{13}C NMR Spectroscopic Data of Compounds **11-14 (**125 MHz)[a]

no.	**11**[b]	**12**[b]	**13**[b]	**14**[c]
1	164.7	164.7	161.7	ND
3	102.1	102.0	137.1	160.7
3a	ND	ND	ND	ND
4	119.9	119.9	111.2	121.0
5	ND	ND	148.5	148.8[d]
6	139.1	139.1	178.8	149.9[d]
6a	117.9	117.9	124.3	115.1
7	144.9	144.9	150.3	128.6
8	130.1	130.1	131.1	131.4
9	125.9	125.9	132.3	ND
9a	127.1	127.1	ND	126.7
9b	123.1	123.1	131.9	127.5
1′	143.6	143.6	142.1	ND
2′	126.3	126.3	127.8	128.2
3′	ND	ND	127.3	128.3
4′	ND	ND	126.9	128.3
5′	ND	ND	127.3	128.3
6′	126.3	126.3	127.8	128.2
1″	102.4	102.6		
2″	73.3	73.3		
3″	76.4	76.4		
4″	69.9	69.9		
5″	76.5	76.5		
6″	61.3	61.3		
OCH_3-3	55.2	55.2		
OCH_3-5				56.9
OCH_3-6				62.0

[a] Carbon assignments based on HSQCAD and gHMBCAD NMR experiments.
[b] Solvent: CD_3OD.
[c] Solvent: $CDCl_3$.
[d] Indicates signals interchangeable.

Table 6. ^{1}H NMR Spectroscopic Data of Compounds **8, 9, 13, 14** (500 MHz)

no.	**11**[a]	**12**[a]	**13**[a]	**14**[b]
3	6.46, s	6.45, s	7.92, s	
4	7.41, s	7.41, s	7.01, s	8.42, s
7				8.54, d (9.0)
8	7.42, m	7.42, m	7.53, d (8.0)	7.61, d (9.0)
9	8.18, d (8.0)	8.18, d (8.0)	8.64, d (8.0)	
2′	7.33, bs	7.33, bs	7.31, m	7.42, m
3′	7.26-7.52, m	7.26-7.52, m	7.39, m	7.49, m
4′	7.26-7.52, m	7.26-7.52, m	7.39, m	7.49, m
5′	7.26-7.52, m	7.26-7.52, m	7.39, m	7.49, m
6′	7.33, bs	7.33, bs	7.31, m	7.42, m
1″	4.77, d (8.0)	4.72, d (8.0)		
2″	2.39, dd (8.0, 9.0)	2.39, dd (8.0, 9.0)		
3″	3.19, m	3.19, m		
4″	2.96, m	2.96, m		
5″	2.91, m	2.91, m		
6″	3.58, m	3.58, m		
1‴	3.45, m	3.45, m		
OH-5	8.54, bs	8.54, bs		
OCH_3-3	3.683, s	3.679, s		
OCH_3-5				4.12, s
OCH_3-6				4.24, s

[a] Solvent: CD_3OD.
[b] Solvent: $CDCl_3$.

An enriched fraction of the methanolic extract of the fruits and of the stems contained compounds **15** and **16**, respectively (λ_{max} = 350–360 nm) (Figures S177–S178, Supporting Information). It became apparent quickly that the NMR spectra of these compounds significantly differed from the PhP-type compounds isolated throughout this study, specifically in terms of the abundance of signals in the region (5–7 ppm), which is usually quite sparse in terms of PhPs (Figures S179–S180, Supporting Information). Through dereplication, it was revealed that the two compounds in question, which had very similar spectra, were of the flavonoid structure class, differing as the mono- and di-*O*-glycoside forms of the known flavonol, quercetin (compounds **15** and **16**, respectively). These structures were supported by the observed molecular ions of 464 amu and 626 amu, respectively. While these do not represent new compounds, they were of considerable interest, as they are the first literature reports of flavonoids being isolated from any member of the genus *Haemodorum*.

A compound isolated during this study was deemed significant with respect to the work by Chen et al., who reported on the metabolic pathways involved in the formation of PBIQs.[12, 17] In these studies, it was reported that 3,5-dihydroxy-6-*O*-glc-7-PBIC (**21**) forms as the result of a non-enzymatic oxidative conversion in the proposed pathway from 3-carboxyl-5-hydroxy-6-*O*-glc-7-PBIC (**22**) to the 7-PBIC anhydride glycoside isolated in that study. A similar motif is seen in the PBIC anhydrides (**14** and **30**) isolated in this current study (Figure S1, Supporting Information).[12, 17] In revealing this metabolic pathway, the study by Chen et al. contributed substantially to our understanding of the biological origin of these compounds.

The results of this current study lend further credibility to that assertion, in that several members of this pathway have been isolated in planta, from another genus in the family Haemodoraceae. In particular, 3-carboxyl-5-hydroxy-6-*O*-glc-7-PBIC (**22**) was isolated from multiple fractions across

the organism, which although initially stable in CD_3OD, began to degrade within two weeks while stored at -20 °C. The 3-carboxyl group moiety reduced first into a 3-hydroxy group moiety in **17**, and over time it steadily converted into a stable saturated C-3 carbon seen in **22**. The isolation of the previously unreported 9-PBIC anhydride aglycone **14** displays a similar anhydride motif to the compound isolated in the study just discussed, although the alternate location of the pendant aromatic ring may also have some interesting ramifications regarding its biosynthetic origins.[12, 17] Further, despite the stability of the 9-PBIC anhydride aglycone **14**, in CD_3OD at -20 °C, it is reported that there is a pH-dependent non-enzymatic relationship between the 7-PBIC anhydride aglycone and the corresponding phenylcarboxynapthoquinone (akin to the phenylcarboxynapthoquinone, **2**), which arose from hydration at pH 7-8. This conversion was not observed in our study, despite the use of H_2O and neutral pH conditions being employed in the HPLC-based isolation but represents an interesting avenue for investigation.

The compounds isolated across the various parts of *H. brevisepalum* (bulbs, stems and fruit) displayed some general distribution trends, shown in Figure S181, Supporting Information. PhPs were distributed throughout the organism only in the glycosylated forms. OBCs were primarily located in the bulbs of the plant in the aglycone form, with only one compound present in the fruits as a glycoside. This trend towards glycosylation in the aerial components is substantiated by the distribution of PBIC compounds, with only aglycones present in the bulbs and only glycosides in the fruit – with a mixture of both forms being present in the stems.

In the biological evaluation procedure implemented, stable pure compounds obtained throughout the study were submitted to one (or more) of two assays. Compounds **2**–**4**, **6**–**9**, **15**–**18**, **21**, **22** and **26** were submitted for antimicrobial screening at The Community for Antimicrobial Drug

Discovery (CO-ADD).[24] Compounds **4**, **6**–**9**, **17** and **21** were submitted to the Parasitology Team at The University of Melbourne for anthelminthic activity screening.

Compounds submitted to CO-ADD antimicrobial assays were evaluated against five bacteria (*Staphylococcus aureus* MRSA, *Escherichia coli*, *Klebsiella pneumoniae*, *Acinetobacter baumanii* and *Pseudomonas aeruginosa*), and two fungi (*Candida albicans* and *Cryptococcus neoformans* var. *grubii*). The compounds submitted were tested at 32 μg/mL with the results of the assays displayed in Figure S134, Supporting Information.

Although none of the compounds tested were deemed biologically active [based on CO-ADD's requirement of inhibition values of >80% and Z-score of >2.5 for either replicate ($n = 2$ on different plates)], all compounds tested showed some selective and varying degrees of antimicrobial activity. While none of the compounds showed any activity against either *E. coli* or *C. neoformans*, the OBC aglycone **3** showed moderate activity with an average inhibition against *S. aureus* MRSA of 58.4%, whereas the glycosylated form of the same compound **26** only displayed an averaged 8.1% inhibition, suggesting a potential structure-activity-relationship (SAR). The moderate activity of compound **3** in the primary screening warranted further hit-confirmation screening to determine MIC values against the same seven microbial species as well as cytotoxicity and hemolysis assays. Subsequently, compound **3** was deemed to be inactive due to it not meeting the CO-ADD required criterion of achieving a MIC of <32 μg/mL. Compounds **6** and **8**, both PhPs, showed slight activity against *C. albicans* with an average inhibition of 29.6% and 38.7%, respectively. These two compounds were similar in that they were both PhP glycones featuring no substitution at C-2 and C-3, as well as having a single hydroxy group moiety on their pendant aromatic ring, although this ring itself differed in its point of attachment at C-7 in **6** and C-8 in **8**.

Compound **6** displayed the broadest activity of the compounds submitted to CO-ADD screening, with slight activity against *S. aureus* MRSA, *P. aeruginosa* and *C. albicans*.

Compounds **4**, **6**–**9**, **17** and **21** were evaluated for anthelminthic activity against exsheathed third-stage larvae (xL3s) of the blood-feeding parasitic nematode *Haemonchus contortus*. Compounds **4**, **6**–**9**, **17**, and **21** were initially tested on the xL3s of *H. contortus* at 20 μM to establish whether any of them inhibited larval motility by ≥70% at 72 h or development after 7 days of compound-exposure. None of these compounds significantly affected larval motility or development.

EXPERIMENTAL SECTION

General Experimental Procedures. All organic solvents used were analytical reagent (AR or GR), UV spectroscopic, or HPLC grade, with Milli-Q water also being used. Optical rotations were carried out using a 1.5 mL cell on a Rudolph Research Analytical Autopol IV automatic polarimeter, set to the Na 589 nm wavelength. UV/vis spectra were recorded on an Agilent Cary 60 spectrophotometer, using ethanol. FTIR spectra were recorded as a film using NaCl disks on a PerkinElmer Spectrum One FTIR spectrometer. ^{1}H (500 MHz), ^{13}C (125 MHz), and 1D NOE spectra were acquired in $CDCl_3$ or CD_3OD, on a 500 MHz Agilent DD2 NMR spectrometer with referencing to solvent signals (δ 7.26 and 77.0 ppm for $CDCl_3$, δ 3.31 and 49.0 for CD_3OD). Two-dimensional NMR experiments performed included gCOSY, HSQCAD, gHMBCAD, and NOESY NMR. Low-resolution ESIMS were obtained on a Micromass Platform II mass spectrometer equipped with an LC-10AD Shimadzu solvent delivery module (50% CH_3CN/H_2O at a flow of 0.2 mL/min), in both the positive- and negative-ionization modes using cone voltages between 20 and 30 V. HRMS were obtained using an Agilent 6540 QTOF MS system (Santa Clara, CA, USA) with a dual nebulizer AJS ESI source. The MS was operated in the negative mode using

the following conditions: nebulizer pressure 45 psi, sheath gas flowrate 10 L/min, gas temperature 300 °C, capillary voltage 4000 V, fragmentor 150 V or 200 V, and skimmer 65 V. The instrument was operated in the extended dynamic range mode with data collected in *m/z* range 100–2000. Test compounds were infused directly into the MS via a kdScientific infusion pump at a static flow rate of 650 µL/h. Alternatively, HRMS were analyzed using a Waters Xevo QTOF mass spectrometer, with an atmospheric solids analysis probe (ASAP) source (probe temperature set to 300 °C, a source temperature set to 80 °C and a sampling cone voltage of 20.0 V). Accurate masses were obtained by lockmass using leucine enkephalin as the reference compound. Silica gel flash chromatography was carried out using Davisil LC35 Å silica gel (40–60 mesh) with a 20% stepwise solvent elution from 100% petroleum spirit (60–80 °C) to 100% CH_2Cl_2, to 100% EtOAc, and finally to 100% MeOH. C_{18} vacuum liquid chromatography was carried out using Davisil 633NC18E C_{18} coated silica gel (200–425 mesh) with a 20% stepwise solvent elution from 100% Milli-Q H_2O to 100% CH_3OH, to 100% CH_2Cl_2, and finally a CH_3OH wash with 0.1% TFA. Sephadex LH-20 size-exclusion chromatography was carried out using Amersham Biosciences Sephadex LH-20 liquid chromatography medium with an isocratic solvent system of 100% CH_3OH. All analytical HPLC analyses and method development were performed on a Dionex P680 solvent delivery system equipped with a PDA100 UV detector (operated using "Chromeleon" software). Analytical HPLC analysis was carried out using either a standard gradient method of 0–2 min 10% CH_3CN/H_2O; 14–24 min 75% CH_3CN/H_2O; 26–30 min 100% CH_3CN; and 32–40 min 10% CH_3CN/H_2O, or else a slight variant of this gradient (detailed below) or an isocratic method (40–80% CH_3CN/H_2O) on an Alltech Alltima HP C_{18} (250 x 4.6) 5 µm column at a flow rate of 1.0 mL/min. Semi-preparative HPLC was carried out on a Varian Prostar 210 solvent delivery system equipped with a Prostar 335 PDA detector (operated using "Star

Workstation" software using an isocratic method (40–80% CH_3CN/H_2O) and an Alltech Alltima C_{18} (250 x 10) 5 µm column at a flow rate of 3.5 mL/min. Solid-phase extraction (SPE) chromatography was conducted with either Alltech Normal Phase "Extract-Clean" Silica SPE cartridges (500 mg, 4.0 mL) or J.T.Baker "Bakerbond" SPE octadecyl (C_{18}) reversed-phase disposable extraction columns (500 mg, 3.0 mL).

Plant Material. *Haemodorum brevisepalum* Benth. was collected in October 2010 from the Arrowsmith River Region, near Eneabba in Western Australia. The plant was collected and identified by Mr. Allan Tinker (plant license SW008335). Voucher specimens with the codes 2010_19a (bulbs), 2010_19b (stems), and 2010_19c (fruits) have been deposited at the School of Science (Applied Chemistry and Environmental Science), RMIT University. In this study, the bulbs (2010_19a), the stems (2010_19b) and the fruits (2010_19c) of *H. brevisepalum* were investigated. Samples were stored at -80 °C from point of collection (2010) until extraction commenced in 2015, crude extracts were stored at -20 °C throughout the isolation process. Samples were first reduced in size with secateurs, then pulverized to a coarse fiber using a conventional blender. The extraction and analysis of the various plant parts commenced in 2015, with the work on the subterranean components completed by 2017 and the aerial components by 2019.

Extraction and Isolation. The bulbs of *H. brevisepalum* (3.20 g, dry weight) were extracted with 3:1 CH_3OH-CH_2Cl_2 (2 L). The stems of *H. brevisepalum* (7.68 g, dry weight) were extracted with 3:1 CH_3OH-CH_2Cl_2 (2 L). The fruits of *H. brevisepalum* (3.11 g, dry weight) were extracted with 3:1 CH_3OH-CH_2Cl_2 (2 L). These three crude extracts were then decanted after 7 days, concentrated under reduced pressure and finally sequentially solvent partitioned (triturated) into CH_2Cl_2- and CH_3OH-soluble extracts, respectively.

The complete details of the extraction and isolation process followed for the new and previously reported compounds in this study are outlined in Figure S182, Supporting Information.

5-Hydroxy-3-methoxy-1H,3H-isochromeno[6,5,4-mna]xanthen-1-one (**1**): Unstable yellow solid; UV (EtOH) λ_{max} (log ε) 231 (5.90), 269 (5.79), 316 (5.67), 439 (5.58) nm; ^{1}H NMR (500 MHz, CD_3OD) and ^{13}C NMR (125 MHz, CD_3OD), see Table 1; ESIMS *m/z* 319 $[M - H]^-$; HRESIMS *m/z* 319.0608 (calcd for $C_{19}H_{11}O_5$, 319.0612).

Methyl 3-methoxy-5-phenyl-1,4-dihydronapthoquinone-8-carboxylate (**2**): Red/brown solid; UV (EtOH) λ_{max} (log ε) 256 (5.90), 337 (5.13), 404 (4.89) nm; ^{1}H NMR (500 MHz, CD_3OD) and ^{13}C NMR (125 MHz, CD_3OD), see Table 2; ESIMS *m/z* 323 $[M + H]^+$; HRESIMS *m/z* 323.0912 (calcd for $C_{19}H_{15}O_5$, 323.0914).

5-Methoxy-1H-naphtho[2,1,8-mna]xanthen-1-one (**3**); Orange plates; did not melt below 360 °C; the UV, NMR spectroscopic and mass spectrometric data were identical to those reported in the literature.[9] ESIMS *m/z* 299 $[M - H]^-$.

(6-((2-((2,5-Dimethoxy-1-oxo-7-phenyl-1H-phenalen-6-yl)oxy)-4,5-dihydroxy-6-(hydroxymethyl)tetrahydro-2H-pyran-3-yl)oxy)-3,4,5-trihydroxytetrahydro-2H-pyran-2-yl)methyl (E)-3-(3,4-dihydroxyphenyl)acrylate (**4**): Red solid; $[\alpha]^{22}_D$ +367 (*c* 0.00088, CH_3OH); UV (EtOH) λ_{max} (log ε) 279 (4.30), 336 (4.21), 465 (3.76) nm; ^{1}H NMR (500 MHz, CD_3OD) and ^{13}C NMR (125 MHz, CD_3OD), see Tables 3 and 4; ESIMS *m/z* 817 $[M - H]^-$; HRESIMS *m/z* 817.2341 (calcd for $C_{42}H_{41}O_{17}$, 817.2349).

6-((4,5-Dihydroxy-6-(hydroxymethyl)-3-((3,4,5-trihydroxy-6-(hydroxymethyl)tetrahydro-2H-pyran-2-yl)oxy)tetrahydro-2H-pyran-2-yl)oxy)-5-hydroxy-2-methoxy-7-phenyl-1H-phenalen-1-one (**5**): Red solid; $[\alpha]^{22}_D$ +152 (*c* 0.00042, CH_3OH); UV (EtOH) λ_{max} (log ε) 278 (5.28), 373

(5.01), 465 (4.87) nm; ^{1}H NMR (500 MHz, CD_3OD) and ^{13}C NMR (125 MHz, CD_3OD), see Tables 3 and 4; ESIMS *m/z* 641 $[M - H]^-$; HRESIMS *m/z* 641.1873 (calcd for $C_{32}H_{34}O_{14}$, 641.1876).

7-(4-Hydroxyphenyl)-5-((3,4,5-trihydroxy-6-(hydroxymethyl)tetrahydro-2H-pyran-2-yl) oxy)-1H-phenalen-1-one (**6**): Red solid; $[\alpha]^{22}_D$ –11 (*c* 0.0025, CH_3OH); UV (EtOH) λ_{max} (log ε) 271 (5.46), 372 (5.25), 437 (5.12) nm; ^{1}H NMR (500 MHz, CD_3OD) and ^{13}C NMR (125 MHz, CD_3OD), see Tables 3 and 4; ESIMS *m/z* 465 $[M - H]^-$; HRESIMS *m/z* 465.1190 (calcd for $C_{25}H_{21}O_9$, 465.1191).

7-(3,4-Dihydroxyphenyl)-5-((3,4,5-trihydroxy-6-(((3,4,5-trihydroxy-6-(hydroxymethyl)tetrahydro-2H-pyran-2-yl)oxy)methyl)tetrahydro-2H-pyran-2-yl)oxy)-2-hydroxy-1H-phenalen-1-one (**7**): Red solid; $[\alpha]^{22}_D$ +29 (*c* 0.00014, CH_3OH); UV (EtOH) λ_{max} (log ε) 269 (5.83), 371 (5.56), 435 (5.44) nm; ^{1}H NMR (500 MHz, CD_3OD) and ^{13}C NMR (125 MHz, CD_3OD), see Tables 3 and 4; ESIMS *m/z* 643 $[M - H]^-$; HRESIMS *m/z* 643.1646 (calcd for $C_{31}H_{31}O_{15}$, 643.1668).

5-Hydroxy-8-(2-hydroxyphenyl)-6-((3,4,5-trihydroxy-6-(hydroxymethyl)tetrahydro-2H-pyran-2-yl)-oxy)1H-phenalen-1-one (**8**): Red solid; $[\alpha]^{22}_D$ +43 (*c* 0.00028, CH_3OH); UV (EtOH) λ_{max} (log ε) 242 (3.50), 257 (3.53), 393 (2.84) nm; ^{1}H NMR (500 MHz, CD_3OD) and ^{13}C NMR (125 MHz, CD_3OD), see Tables 3 and 4; ESIMS *m/z* 465 $[M - H]^-$; HRESIMS *m/z* 465.1199 (calcd for $C_{25}H_{21}O_9$, 465.1191).

2-Hydroxy-8-(2-hydroxyphenyl)-6-((3,4,5-trihydroxy-6-(hydroxymethyl)tetrahydro-2H-pyran-2-yl)oxy)-1H-phenalen-1-one (**9**): Red solid; $[\alpha]^{22}_D$ –146 (*c* 0.002, CH_3OH); UV (EtOH) λ_{max} (log ε) 248 (5.57), 289 (5.38), 457 (5.02) nm; ^{1}H NMR (500 MHz, CD_3OD) and ^{13}C NMR (125 MHz, CD_3OD), see Tables 3 and 4; ESIMS *m/z* 465 $[M - H]^-$; HRESIMS *m/z* 465.1191 (calcd for $C_{25}H_{21}O_9$, 465.1167).

8-(2-Hydroxyphenyl)-5,6-bis((3,4,5-trihydroxy-6-(hydroxymethyl)tetrahydro-2H-pyran-2-yl)oxy)-1H-phenalen-1-one (**10**): Red solid; UV (EtOH) λ_{max} 257, 283 sh, 416 nm; ^{1}H NMR (500 MHz, CD_3OD) and ^{13}C NMR (125 MHz, CD_3OD), see Tables 3 and 4; ESIMS *m/z* 663 $[M + H + Cl]^+$; HRESIMS *m/z* 663.1489 (calcd for $C_{31}H_{32}ClO_{14}$, 663.1475).

5-Hydroxy-(3R/S)-3-methoxy-7-phenyl-6-((3,4,5-trihydroxy-6-(hydroxymethyl)tetrahydro-2H-pyran-2-yl)oxy)-1H,3H-benzo[de]isochromen-1-one (**11**): Orange solid; UV (EtOH) λ_{max} 252, 334, 367 nm; ^{1}H NMR (500 MHz, CD_3OD) and ^{13}C NMR (125 MHz, CD_3OD), see Tables 5 and 6; ESIMS *m/z* 483 $[M - H]^-$; HRESIMS *m/z* 483.1294 (calcd for $C_{25}H_{23}O_{10}$, 483.1297).

5-Hydroxy-(3R/S)-3-methoxy-7-phenyl-6-((3,4,5-trihydroxy-6-(hydroxymethyl)tetrahydro-2H-pyran-2-yl)oxy)-1H,3H-benzo[de]isochromen-1-one (**12**): Orange solid; UV (EtOH) λ_{max} 252, 334, 367 nm; ^{1}H NMR (500 MHz, CD_3OD) and ^{13}C NMR (125 MHz, CD_3OD), see Tables 5 and 6; ESIMS *m/z* 483 $[M - H]^-$; HRESIMS *m/z* 483.1294 (calcd for $C_{25}H_{23}O_{10}$, 483.1297).

5-Amino-7-phenyl-1H,6H-benzo[de]isochromene-1,6-dione (**13**): Orange solid; UV (EtOH) λ_{max} (log ε) 204 (5.31), 244 (4.99), 269 (4.86), 327 (4.61), 446 (4.42) nm; ^{1}H NMR (500 MHz, CD_3OD) and ^{13}C NMR (125 MHz, CD_3OD), see Tables 5 and 6; ESIMS *m/z* 288 $[M - H]^-$; HRESIMS *m/z* 288.0662 (calcd for $C_{18}H_{10}NO_3$, 288.0666).

5,6-Dimethoxy-9-phenyl-1H,3H-benzo[de]isochromene-1,3-dione (**14**): Orange solid; UV (EtOH) λ_{max} (log ε) 255 (5.06), 307 (4.27), 339 (4.11) nm; ^{1}H NMR (500 MHz, CD_3OD) and ^{13}C NMR (125 MHz, CD_3OD), see Tables 5 and 6; ESIMS *m/z* 335 $[M + H]^+$; HRESIMS *m/z* 335.0916 (calcd for $C_{20}H_{15}O_5$, 335.0914).

2-(3,4-Dihydroxyphenyl)-5,7-dihydroxy-3-((3,4,5-trihydroxy-6-(hydroxymethyl)tetrahydro-2H-pyran-2-yl)oxy)-4H-chromen-4-one (**15**); Red/brown solid; The UV, NMR spectroscopic and mass spectrometric data were identical to those reported in the literature;[25] ESIMS *m/z* 463 $[M - H]^-$.

2-(3,4-Dihydroxyphenyl)-5,7-dihydroxy-3-((3,4,5-trihydroxy-6-(((3,4,5-trihydroxy-6-(hydroxymethyl)tetrahydro-2H-pyran-2-yl)oxy)methyl)tetrahydro-2H-pyran-2-yl)oxy)-4H-chromen-4-one (**16**); Red/brown solid; The UV, NMR spectroscopic and mass spectrometric data were identical to those reported in the literature;[26] ESIMS *m/z* 425 $[M - H]^-$.

5-Hydroxy-7-phenyl-6-((3,4,5-trihydroxy-6-(hydroxymethyl)tetrahydro-2H-pyran-2-yl)oxy)-1H,3H-benzo[de]isochromen-1-one (**17**): Orange solid; the UV, NMR spectroscopic and mass spectrometric data were identical to those reported in the literature;[16] ESIMS *m/z* 453 $[M - H]^-$.

Compound **17** was derivatized chemically to form the new acetylated derivative **18**. Thus, 0.6 mg of **17** was dried prior to the addition of 0.6 mL of pyridine (C_5H_5N), then stirred for 1 min prior to the addition of 0.6 mL of acetic anhydride [$(CH_3CO)_2O$]. This solution was stirred at room temperature (25 °C) overnight, then **18** was evaporated to dryness under an inert nitrogen stream.

2-((5-Acetoxy-1-oxo-7-phenyl-1H,3H-benzo[de]isochromen-6-yl)oxy)-6-(acetoxymethyl)tetrahydro-2H-pyran-3,4,5-triyl triacetate (**18**): Orange solid; $[\alpha]^{22}_D$ –33 (*c* 0.0012, CH_3OH); UV (EtOH) λ_{max} (log ε) 259 (5.59), 333 (5.06), 365 (5.02) nm; ^{1}H NMR (500 MHz, C_2D_6OS) δ 8.28 (1H, d, *J* = 7.5 Hz, H-9), δ 7.01-7.47 (3H, m, H-3'-5'), δ 7.52 (1H, s, H-4), δ 7.51 (1H, d, *J* = 7.5 Hz, H-8), δ 7.27 (1H, bs, H-2′/6′), δ 7.03 (1H, bs, H-2′/6′), δ 5.84 (1H, d, *J* = 15.0 Hz, H-3a), δ 5.80 (1H, d, *J* = 15.0 Hz, H-3b), δ 5.12 (1H, dd, *J* = 9.0, 9.5 Hz, H-3″), δ 5.05 (1H, d, *J* = 7.5 Hz, H-1″), δ 4.50 (1H, dd, *J* = 9.5, 10.0 Hz, H-3″), δ 4.06 (1H, dd, *J* = 6.0, 12.5, H-6″a), δ 3.69 (1H, m, H-2″), δ 3.67 (1H, m, H-5″), δ 3.50 (1H, m, H-6″b), δ 2.34 (3H, s, $COCH_3$-5), δ 1.90 (3H, s, $COCH_3$-2″), δ 1.88 (3H, s, $COCH_3$-4″), δ 1.87 (3H, s, $COCH_3$-3″), δ 1.70 (3H, s, $COCH_3$-6″); ^{13}C NMR (500 MHz, C_2D_6OS) δ 170.03 (C, C=O-3″), δ 169.97(C, C=O-6″), δ 169.6 (C, C=O-4″), δ 168.6 (C, C=O-2″), δ 168.5 (C, C=O-5), δ 163.7 (C, C-1), δ 145.4 (C, C-7), δ 142.7 (C, C-1′), δ 141.9 (C, C-6), δ 140.9 (C, C-5), δ 131.6 (CH, C-8), δ 128.5 (CH, C-9), δ

128.1 (C, C-9b), δ 127.1 (C, C-9a), δ 127.0-127.2 (3CH, C-3′-5′), δ 127.0 (2CH, C-2′/5′), δ 126.4 (C, C-3a), δ 119.81 (C, C-6a), δ 119.78 (CH, C-4), δ 99.6 (CH, C-1″), δ 72.2 (CH, C-3″), δ 71.4 (CH, C-2″), δ 70.6 (CH, C-5″), δ 67.9 (CH, C-4″), δ 61.5 (CH_2, C-6″), δ 21.2 (C, C=O-CH_3-5), δ 20.8 (C, C=O-CH_3-2″), δ 20.75 (C, C=O-CH_3-3″), δ 20.72 (C, C=O-CH_3-4″), δ 20.5 (C, C=O-CH_3-6″); ESIMS (negative mode) *m/z* 621 $[M - Ac]^-$; ESIMS (positive mode) *m/z* 687 $[M + Na]^+$.

2,5-Dihydroxy-7-phenyl-6-((3,4,5-trihydroxy-6-(hydroxymethyl)tetrahydro-2H-pyran-2-yl)oxy)-1H-phenalen-1-one (**19**): Red solid; the UV, NMR spectroscopic and mass spectrometric data were identical to those reported in the literature;[11, 20] ESIMS *m/z* 465 $[M - H]^-$.

Dilatrin [*5-Hydroxy-2-methoxy-7-phenyl-6-((3,4,5-trihydroxy-6-(hydroxymethyl)tetrahydro-2H-pyran-2-yl)oxy)-1H-phenalen-1-one*] (**20**): Red solid; the UV, NMR spectroscopic and mass spectrometric data were identical to those reported in the literature;[7] ESIMS m/z 479 $[M - H]^-$.

(3R/S)-3,5-Dihydroxy-7-phenyl-6-((3,4,5-trihydroxy-6-(hydroxymethyl)tetrahydro-2H-pyran-2-yl)oxy)-1H,3H-benzo[de]isochromen-1-one (**21**): Orange solid; the NMR spectroscopic and mass spectrometric data were identical to those reported in the literature;[18] $[\alpha]^{22}_D$ +49 (*c* 0.00026, CH_3OH); ESIMS *m/z* 469 $[M - H]^-$; HRESIMS *m/z* 469.1143 (calcd for $C_{24}H_{21}O_{10}$, 469.1140).

5-Hydroxy-(3R/S)-3-carboxy-7-phenyl-6-((3,4,5-trihydroxy-6-(hydroxymethyl)tetrahydro-2H-pyran-2-yl)oxy)-1H,3H-benzo[de]isochromen-1-one (**22**): Orange solid; the UV, NMR spectroscopic and mass spectrometric data were identical to those reported in the literature;[19] $[\alpha]^{22}_D$ +72 (*c* 0.0001, CH_3OH); ESIMS *m/z* 497 $[M - H]^-$.

5-Hydroxy-1H-naphtho[2,1,8-mna]xanthen-1-one (**23**): Purple solid; the UV, NMR spectroscopic and mass spectrometric data were identical to those reported in the literature;[9] ESIMS *m/z* 285 $[M - H]^-$.

5-Hydroxy-2-methoxy-1H-naphtho[2,1,8-mna]xanthen-1-one (**24**): Purple solid; the UV, NMR spectroscopic and mass spectrometric data were identical to those reported in the literature;[9] ESIMS *m/z* 315 $[M - H]^-$.

2,5-Dimethoxy-1H-naphtho[2,1,8-mna]xanthen-1-one (**25**): Purple solid; the UV, NMR spectroscopic and mass spectrometric data were identical to those reported in the literature;[9] ESIMS *m/z* 329 $[M - H]^-$.

5-Methoxy-11-((3,4,5-trihydroxy-6-(hydroxymethyl)tetrahydro-2H-pyran-2-yl)oxy)-1H-naphtho[2,1,8-mna]xanthen-1-one (**26**): Purple solid; the UV, NMR spectroscopic and mass spectrometric data were identical to those reported in the literature;[8] ESIMS *m/z* 479 $[M + H]^+$.

Haemodordiol [*5,6-Dihydroxy-(3R/S)-3-methoxy-7-phenyl-1H,3H-benzo[de]isochromen-1-one*] (**27**): Orange solid; the UV, NMR spectroscopic and mass spectrometric data were identical to those reported in the literature;[9] ESIMS *m/z* 321 $[M - H]^-$.

6-Hydroxy-(3R/S)-3,5-dimethoxy-7-phenyl-1H,3H-benzo[de]isochromen-1-one (**28**): Orange solid; the UV, NMR spectroscopic and mass spectrometric data were identical to those reported in the literature;[17, 18] ESIMS *m/z* 365 $[M - H]^-$.

5-Hydroxy-(3R/S)-3,6-dimethoxy-7-phenyl-1H,3H-benzo[de]isochromen-1-one (**29**): Orange solid; the UV, NMR spectroscopic and mass spectrometric data were identical to those reported in the literature;[16, 27] ESIMS *m/z* 365 $[M - H]^-$.

Haemodorone [*5-Hydroxy-6-methoxy-7-phenyl-1H,3H-benzo[de]isochromene-1,3-dione*] (**30**): Orange solid; the UV, NMR spectroscopic and mass spectrometric data were identical to those reported in the literature;[7, 8] ESIMS *m/z* 319 $[M - H]^-$.

X-Ray Crystallographic Analysis of 5-methoxy-1*H*-naphtho[2,1,8-*mna*]xanthen-1-one (3). An orange plate-like crystal of $C_{20}H_{12}O_3.H_2O$, M = 318.31, approximate dimensions 0.090 mm ×

0.040 mm × 0.009 mm, was used for the X-ray crystallographic analysis at the Australian Synchrotron MX2 beamline,[28] using radiation with wavelength 0.9184 Å. The integration of the data using a monoclinic unit cell yielded a total of 12757 reflections in the range $2.16° < \theta < 30.33°$ of which 1752 were independent (completeness = 88.5%, R_{int} = 0.1265%). The final cell constants were a = 4.799(1) Å, b = 17.338(4) Å, c = 17.021(3) Å, β = 90.85(3)°, V = 1416.1(5) Å3, T = 100.0(2) K. The structure was solved by direct methods and difference Fourier synthesis, and was refined on the F2 (SHELXL) integrated within the WinGX software package,[29, 30] in the space group *P21/c*, with Z = 4, μ = 0.19 mm^{-1}. The final R_1 values were 0.0679 ($I>2\sigma(I)$), 1419 data). The final $wR(F^2)$ values were 0.2059 (all data). The goodness of fit on F^2 was 1.055. The thermal ellipsoid plot was generated using the program Mercury.[31] The crystallographic data for the structure of **3** were deposited at the Cambridge Crystallographic Data Centre (deposition number: CCDC 2077693). Copies of these data can be obtained free of charge on application at the following address: www.ccdc.cam.ac.uk or from the Cambridge Crystallographic Data Centre (12 Union Road, Cambridge CB21EZ, UK; fax (+44) 1223-336-033; or deposit@ccdc.cam.ac.uk).

Antimicrobial Activity Assay. The antimicrobial activity testing was conducted through collaboration with the Community for Open Antimicrobial Drug Discovery (CO-ADD), for experimental details see S183, Supporting Information**.**

Anthelmintic Activity Assay. The anthelmintic activity testing was conducted at the University of Melbourne (see S184, Supporting Information).[32] In brief, compounds were screened at a concentration of 20 μM on exsheathed third-stage larvae (xL3s) of *Haemonchus contortus* in 96-well microtiter plates (Corning, NY, USA) containing 300 xL3s per well. A compound was recorded as having anthelmintic activity if it reduced xL3 motility by ≥70% after 72 h of compound exposure and/or inhibited larval development at 7 days.

ASSOCIATED CONTENT

Supporting Information

The Supporting Information is available free of charge at:

Tabulated 2D NMR data of new compounds, relevant in-text figures, X-Ray crystallographic atomic coordinates and hydrogen bonding details for compound **3**, tabulated antimicrobial data for compounds **2**–**4**, **6**–**9**, **15**–**18**, **21**, **22**, **26** (CO-ADD), extracted 2D HPLC-PDA chromatograms, ^{1}H NMR spectra, 2D NMR spectra, NOE NMR spectra, HRESIMS of new compounds, graphical figures representing compound class distribution, experimental details of extraction, isolation, antimicrobial activity testing and anthelmintic activity testing.

AUTHOR INFORMATION

Complete contact information is available at:

Notes

The authors declare no competing financial interest.

ACKNOWLEDGMENTS

The antimicrobial screening performed by CO-ADD (The Community for Antimicrobial Drug Discovery) was funded by the Wellcome Trust (UK) and The University of Queensland (Australia). E. O. Norman would like to acknowledge the financial support awarded under the

Research Stipend Scholarship (RSS) scheme provided by the Australian Government via RMIT University. The anthelmintic discovery project was funded by Yourgene Health Singapore Pty. Ltd. and the Australian Research Council (ARC Grant number LP190101209; R. B. Gasser). J. M. White acknowledges funding from the ARC LIEF Scheme (grant number LE170100065) This research was undertaken in part using the MX2 beamline at the Australian Synchrotron, part of ANSTO, and made use of the Australian Cancer Research Foundation (ACRF) detector.

REFERENCES

(1) Byng, J. W.; Chase, M. W.; Christenhusz, M. J. M.; Fay, M. F.; Judd, W. S.; Mabberley, D. J.; Sennikov, A. N.; Soltis, D. E.; Soltis, P. S.; Stevens, P. F. *Bot. J. Linn. Soc.* **2016,** *181*, 1-20.

(2) Norman, E. O.; Lever, J.; Brkljaca, R.; Urban, S. *Nat. Prod. Rep.* **2019,** *36*, 753-768.

(3) Lassak, E. V.; McCarthy, T. In *Australian Medicinal Plants*; Methuen Australia Pty Ltd.: Sydney, Australia 1983.

(4) Lazzaro, A.; Coromina, M.; Martí, C.; Flors, C.; Izquierdo, L. R.; Grillo, T. A.; Luis, J. G.; Nonell, S. *Photochem. Photobiol.* **2004,** *3*, 706-710.

(5) Hidalgo, W.; Duque, L.; Saez, J.; Arango, R.; Gil, J.; Rojano, B.; Schneider, B.; Otalvaro, F. *J. Agric. Food Chem.* **2009,** *57*, 7417-7421.

(6) Magiorakos, A. P.; Srinivasan, A.; Carey, R. B.; Carmeli, Y.; Falagas, M. E.; Giske, C. G.; Harbarth, S.; Hindler, J. F.; Kahlmeter, G.; Olsson-Liljequist, B.; Paterson, D. L.; Rice, L. B.; Stelling, J.; Struelens, M. J.; Vatopoulos, A.; Weber, J. T.; Monnet, D. L. *Clin. Microbiol. Infect.* **2012,** *18*, 268-281.

(7) Dias, D. A.; Goble, D. J.; Silva, C. A.; Urban, S. *J. Nat. Prod.* **2009,** *72*, 1075-1080.

(8) Urban, S.; Brkljaca, R.; White, J. M.; Timmers, M. A. *Phytochemistry* **2013,** *95*, 351-359.

(9) Brkljaca, R.; Urban, S. *J. Nat. Prod.* **2015,** *78*, 1486-1494.

(10) Keith, D. *Proc. Linn. Soc. N.S.W.* **1996,** *116*, 37-78.

(11) Chen, Y.; Paetz, C.; Menezes, R. C.; Schneider, B. *Phytochemistry* **2017,** *133*, 15-25.

(12) Chen, Y.; Paetz, C.; Schneider, B. *Phytochemistry* **2019,** *159*, 30-38.

(13) Castleden, I. R.; Engelhardt, L. M.; Hall, S. R.; White, A. H. *Aust. J. Chem.* **1984,** *37*, 1763-1768.

(14) Kazuma, K.; Noda, N.; Suzuki, M. *Phytochemistry* **2003,** 62, 229-237.

(15) Nawwar, M. A. M.; El-Mousallamy, A. M. D.; Barakat, H. H. *Phytochemistry* **1989,** *28*, 1755-1757.

(16) Fang, J.; Paetz, C.; Holscher, D.; Munde, T.; Schneider, B. *Phytochemistry Lett.* **2011,** *4*, 203-208.

(17) Chen, Y.; Paetz, C.; Schneider, B. *J. Nat. Prod.* **2018,** *81*, 879-884.

(18) Fang, J.; Kai, M.; Schneider, B. *Phytochemistry* **2012,** *81*, 144-152.

(19) Opitz, S.; Holscher, D.; Oldham, N. J.; Bartram, S.; Schneider, B. *J. Nat. Prod.* **2002,** *65*, 1122-1130.

(20) Dora, G.; Xie, X.-Q.; Edwards, J. M. *J. Nat. Prod.* **1993,** *56*, 2029-2033.

(21) Brkljaca, R.; White, J. M.; Urban, S. *J. Nat. Prod.* **2015,** *78*, 1600-1608.

(22) Brkljaca, R.; Schneider, B.; Hidalgo, W.; Otalvaro, F.; Ospina, F.; Lee, S.; Hoshino, M.; Fujita, M.; Urban, S. *Molecules* **2017,** *22*, 211-220.

(23) Schneider, B. *Phytochemistry Lett.* **2017,** *21*, 104-108.

(24) Blaskovich, M. A.; Zuegg, J.; Elliot, A. G.; Cooper, M. A. *ACS Infect. Dis.* **2015,** *1*, 285-287.

(25) Kunert, O.; Haslinger, E.; Schmid, M. G.; Reiner, J.; Bucar, F.; Mulatu, E.; Abebe, D.; Debella, A. *Monatsh. Chem.* **2000,** *131*, 195-204.

(26) Amani, M. D. *Phytochemistry* **1998,** *48*, 759-761.

(27) Opitz, S.; Schneider, B. *Phytochemistry* **2003,** *62*, 307-312.

(28) McPhillips, T. M.; McPhillips, S. E.; Chiu, H. J.; Cohen, A. E.; Deacon, A. M.; Ellis, P. J.; Garman, E.; Gonzalez, A.; Sauter, N. K.; Phizackerley, R. P.; Soltis, S. M.; Kuhn, B. *J. Synchrotron Rad.* **2002,** *9*, 401-406.

(29) Sheldrick, G. *Acta Cryst.* **2015,** *71*, 3-8.

(30) Farrugia, L. J. *J. Appl. Cryst.* **1990,** *32*, 837-838.

(31) Macrae, C. F.; Bruno, I. J.; Chisholm, J. A.; Edgington, P. R.; McCabe, P.; Pidcock, E.; Rodriguez-Monge, L.; Taylor, R.; van de Streek, J.; Wood, P. A. *J. Appl. Cryst.* **2008,** *41*, 466-470.

(32) Preston, S.; Jabbar, A.; Nowell, C.; Joachim, A.; Ruttkowski, B.; Baell, J. *Int. J. Parasitol.* **2015,** *5*, 333-343.

Haemodorum brevisepalum